4、 外语能力证书

全国大学英语四级考试
成绩报告单

CET®

姓　　名：薛维兵
学　　校：巢湖学院
院　　系：机械工程学院
身份证号：

笔　试

准考证号：
考试时间：2020年12月

总分	听力 (35%)	阅读 (35%)	写作和翻译 (30%)
475	187	159	129

口　试

准考证号：__

等级	__

考试时间：__

成绩报告单编号：

教育部考试中心
证书专用章

5、 学术能力证明材料

Innovative bio-based bamboo adhesive: Performance breakthrough through the host-guest interaction of cyclodextrin and adamantane

Weibing Xue [a,1], Rui Zhao [a,1], Tongda Liu [a,*], Xin Ran [a], Rong Liu [a], Tonghua Lu [c], Renzhong Wei [c], Guanben Du [a,b], Jun Li [a,*], Long Yang [a,b,**]

[a] Yunnan Province Key Lab of Wood Adhesives and Glued Products, International Joint Research Center for Biomass Materials, School of Materials and Chemical Engineering, Southwest Forestry University, Kunming 650224, China
[b] Key Laboratory for Forest Resources Conservation and Utilization in the Southwest Mountains, Ministry of Education, Southwest Forestry University, Kunming 650224, China
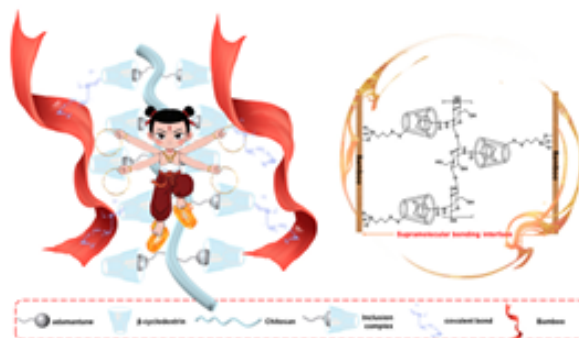[c] Treezo New Material Science and Technology Group Co., Ltd., Hangzhou, Zhejiang 311100, China

HIGHLIGHTS

- Host-guest recognition was applied to the bonding technology field.
- Development of a supramolecular bonding interface (SBI).
- Bonding performance realized break-through by constructing SBI.
- The strategy of building SBI to enhance performance is universally applicable.
- This work provides idea for the innovative development of bonding technology.

GRAPHICAL ABSTRACT

Construction of supramolecular bamboo bonding interface by cyclodextrins and adamantane through host-guest recognition interactions.

ARTICLE INFO

ABSTRACT

Recently, the use of agricultural, forestry, and fishery residues and wastes to develop green and environmentally friendly bio-based adhesives has gradually become the industry development trend and is an effective technical path to implement energy saving, environmental protection, and achieve sustainable development. The present work cleverly leverages the unique advantages of bio-based chitosan and 1-adamantane carboxylic acid to develop an innovative adamantane-chitosan bamboo adhesive through an amidation reaction. Meanwhile, sulfhydryl-functionalized cyclodextrins were prepared, and the cyclodextrin host molecules were successfully anchored to the bamboo surface through bridging 3-mercaptopropyltrimethoxysilane. During the bonding

process, the adamantane guest molecules on the adhesive and the cyclodextrin host molecules on the bamboo surface were subject-guest recognized, resulting in the construction of a host-guest chemical bonding interface to achieve a breakthrough in bonding performance. The dry, hot, and boiling water strength of the bamboo bonded specimens without the formation of supramolecular bonding interface were 7.8, 6.4, and 4.9 MPa, respectively. After constructing the supramolecular bonding interface, the dry, hot, and boiling water strengths were enhanced by 37.2 %, 12.5 %, and 30.6 % to 10.7 MPa, 7.2 MPa, and 6.4 MPa, respectively. The results demonstrated that the host-guest recognition in the supramolecular bonding interface effectively enhanced the bonding performance. The present work utilizes biomass materials and supramolecular forces to achieve high-performance bonding of substrates, breaking the bonding performance enhancement mechanism of traditional adhesives and providing a new way for technological innovation in the field of bonding.

1. Introduction

Bamboo, with its fast growth rate and high yield, is a renewable resource with great potential. It is one of the earliest natural materials developed and utilized by mankind, carrying the memory of civilization spanning thousands of years [1,2]. With the deepening of the global concept of sustainable development, bamboo is undergoing a paradigm shift from a traditional material to a modern strategic resource [3]. Its ecological advantage of sequestering up to 24 tons of carbon per hectare per year makes it a natural solution to climate change [4]. Modern materials science has improved the strength of bamboo to the level of 800 MPa through technological breakthroughs such as hot-pressing modification [5,6] and bamboo fiber composites [7,8], and developed new engineering materials such as bamboo integrative materials and bamboo entangled composites, which are widely used in high-end fields such as green buildings and transportation equipment [9,10]. The development of bamboo composites has the potential to facilitate the efficient utilization of bamboo resources, thereby reducing waste and achieving sustainable development [11].

In the process of preparing bamboo composites, adhesives play an indispensable role, which directly affects the performance and application scope of bamboo composites [12–14]. Currently, the research on adhesives is showing remarkable trends in many aspects [15]. From the environmental point of view, with the increasingly stringent environmental regulations and the growing awareness of consumers of environmental protection, research and development of green and environmentally friendly adhesives has become a general trend [16–18]. Conventional adhesives often contain volatile organic compounds (VOCs), which not only pollute the environment but can also be hazardous to human health. Therefore, the research and development of low-VOC, biomass-based adhesives has become a hotspot, aiming to reduce harmful emissions during production and use and to reduce the negative impact on the environment [19,20]. Among the many green adhesives, biomass adhesives stand out with their unique advantages. Firstly, the raw materials of biomass adhesives come from renewable biomass resources, such as plant fibers [21], starch [22], proteins [23], etc. These resources are abundant and sustainable, which greatly reduces the dependence on fossil resources and is in line with the concept of sustainable development. Secondly, biomass adhesives usually have good biodegradability and can be gradually decomposed in the natural environment, which will not cause long-term environmental pollution problems as traditional adhesives [24,25]. From a health perspective, biomass adhesives are generally free of harmful chemicals and do not release toxic gases such as formaldehyde during use, which is more protective of the user's health and indoor air quality [26]. However, some biomass adhesives typically exhibit relatively poor bonding properties. Consequently, the ability to ensure the mechanical properties of bamboo composites while achieving a balance between environmental protection and performance has become a key research direction in the field of biomass-based adhesives [27,28].

In actual bonding, effective bonding is often not realized by a single bonding mechanism. Instead, multiple mechanisms function collectively and reciprocally, thereby ensuring a harmonious and synergistic outcome. The overall bonding effect and bonding strength between the adhesive and the adherend are jointly determined by the performance of the adhesive itself as well as the forces acting between the adhesive and the substrate [29]. The research on the interaction with adhesives is relatively mature, while comparatively little research has been conducted on the interaction between adhesives and substrates. It is an effective research idea to enhance the covalent chemical cross-linking between the adhesive and the substrate to realize the enhancement of the adhesive properties. Liu et al. achieved enhanced bonding performance by preparing an aminated cellulose as an adhesive while oxidizing the poplar surface and constructing a covalent chemical bonding interface through a chemical reaction between the adhesive and the substrate [30]. Liu et al. aminated wood, while using branched epoxy compounds reacted with aminated cellulose to prepare an adhesive with strong cohesion, branched epoxy compounds as a bond, a sandwich-type wood chemical bonding interface was constructed between the adhesive and the wood surface, to investigate the effects of adhesive cohesion and interfacial force on the bonding properties, respectively [31]. Kang et al. constructed an epoxy-functionalized bamboo surface in which the epoxy groups on the bamboo surface were chemically cross-linked with the amino groups in the cellulose-based adhesive to form a covalent bonding interface, achieving improved bonding properties [32]. Adhesive performance enhancement can also be achieved through non-covalent forces at the interface. Su et al. modified bamboo with aldehyde/carboxylic functionalization, using only chitosan as an adhesive and achieved performance enhancement of bamboo composites through non-covalent/covalent interactions such as electrostatic forces and hydrogen bonding at the interface [33]. Liu et al. achieved the enhancement of poor to robust water resistance of three-layer plywood by modulating multiple covalent/non-covalent forces at the interface [34].

In the field of supramolecular chemistry, researchers have studied the host-guest interactions of cyclodextrins with adamantanes, and there is a large number of related academic literature and research reports [35–38]. The present work prepared a biomass-based adhesive with adamantane guest molecules by cross-linking chitosan and 1-adamantane carboxylic acid through an amidation reaction, while a bamboo surface with cyclodextrin host molecules was prepared by anchoring mercapto-β-cyclodextrin to the bamboo surface through 3-mercaptopropyltrimethoxysilane (KH-590). During the bonding process, the host-guest recognition between adamantane and cyclodextrin was employed to form a supramolecular bonding interface to achieve further enhancement of the bonding performance. The present work realized the use of host-guest recognition interaction for enhancing the bonding performance of composites, further verified the feasibility of supramolecular interaction force to enhance the bonding performance of composites, broke the bonding concept of traditional adhesives, and expanded the idea of high-performance composites preparation.

2. Materials and methods

2.1. Materials and chemicals

Chitosan (CS), β-Cyclodextrin (β-CD), tosyl chloride, ammonium chloride (NH$_4$Cl), Thiourea (TU), Trichloroethylene (TCE), 1-

3. Results and discussion

3.1. Characterization of CS-AD adhesive

An adamantane-modified chitosan-based adhesive (CS-AD adhesive) was prepared by a simple amidation reaction using chitosan and 1-adamantane carboxylic acid. Schematic diagram of the preparation process and proposed chemical structure of CS-AD adhesive are shown in Fig. 1a and photos of the prepared CS-AD adhesive are shown in Fig. 1b. The chemical structure changes of CS-AD adhesive were characterized by FT-IR as shown in Fig. 1c. The CS-AD sample has a broad peak near

3300–3500 cm^{-1} attributed to the stretching vibration of O-H and N-H [31]. The signals at 1650 cm^{-1}, 1558 cm^{-1}, and 1275 cm^{-1} correspond to the stretching vibration of C=O, the bending vibration of N-H and the stretching vibration of C-N, respectively. Thus, it is proved that CS reacts successfully with Hadc to form an amide bond (NH-C=O), i.e., the successful preparation of CS-AD adhesive. The CS-AD samples were further analyzed by XPS and the results are shown in Fig. 1d-g. The presence of amide (NH-C=O) bonding signals in the N 1 s high-resolution spectra also indicates the successful occurrence of the amidation reaction [34].
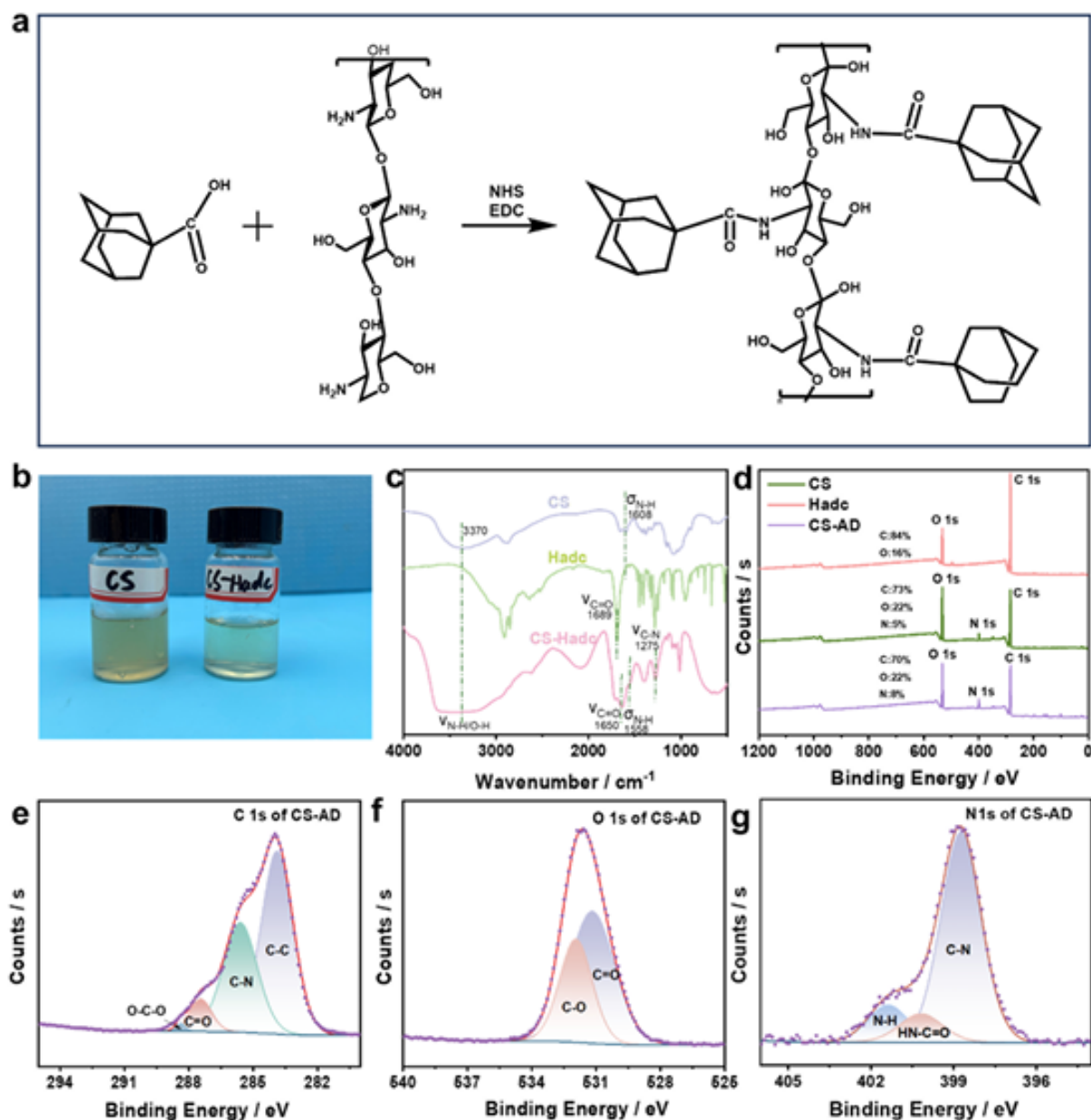

Fig. 1. (a) Schematic diagram of the preparation process and proposed chemical structure of CS-AD adhesive. (b) The photo of CS-AD adhesive. (c) FTIR spectra of CS, Hadc, and CS-AD. (d) XPS spectra of CS, Hadc, and CS-AD. (e-g) High-resolution spectra of C 1 s, O 1 s, and N 1 s of CS-AD.

adamantane carboxylic acid (Hadc), 1-(3-Dimethylaminopropyl)-3-ethylcarbodiimide (EDC), N-Hydroxy succinimide (NHS), acetic acid, methanol, Sodium hydroxide (NaOH), hydrogen peroxide (H_2O_2) and 3-mercaptopropyltrimethoxysilane (KH-590) were obtained from Shanghai Adamas Reagent Co., Ltd. (Shanghai, China). Bamboo was purchased from Kunming, China. Wood (poplar and beech) was purchased from Shandong, China. All reagents are used directly without further purification.

2.2. Preparation of chitosan-based adhesives grafted with adamantane (CS-AD)

The chitosan, acetic acid, and deionized water were mixed according to the mass ratio of 3:1:50 and stirred at room temperature for 3–6 h to homogenize. Then dissolve adamantane carboxylic acid, NHS, and EDC into methanol according to the mass ratio of 6:1:1, and after heating at 60 °C for 30 min, add into the dissolved chitosan solution, and react at 60 °C for 8–10 h to obtain CS-AD adhesive, which is a light-yellow oily fluidity liquid.

2.3. Preparation of the host compound 6-mercapto-β-cyclodextrin (6-SH-β-CD)

The 30.0 g of β-cyclodextrin and 7.8 g of tosyl chloride were added to 720 mL of deionized water and stirred for 2–3 h. After that, 2.5 mol/L NaOH aqueous solution of 120 mL was added, and stirring was continued for about 30 min. The insoluble material was removed by filtration, and the filtrate was collected. About 36.0 g of NH_4Cl was added to the solution and the pH was adjusted to 8. The solution was placed in a refrigerator for 12 h and then filtered to obtain a white insoluble solid. After washing the solid with deionized water 3 times, it was recrystallized with water to obtain bright white flaky crystals, which were dried and dried under vacuum at 50 °C to obtain 6.0 g of white powdery solid is the mono-6-O-tosyl-β-CD.

4.0 g of mono-6-O-tosyl-β-CD and 4.4 g of thiourea were added to 200 mL of mixed solvent (methanol: water = 80:20) and refluxed at room temperature for 2 days. The solvent was removed by distillation under reduced pressure and the residue was added to 60 mL of methanol and stirred for 1.5 h, then immersed for 1 day and filtered to obtain a white solid. The solid obtained was dissolved in 140 mL of 10 % NaOH solution and placed at the constant temperature range of 50 °C for 5 h, then the pH value was adjusted to 2 with 10 % HCl solution, and 10 mL of trichloroethylene was added, and stirred for 1 day. The white solid was precipitated, and filtered, and the solid obtained was dried in vacuum at 50 °C, and 2.2 g of white powdery solid was obtained, which was 6-mercapto-β-cyclodextrin (6-SH-β-CD).

2.4. Preparation of activated bamboo surface (ABS)

The obtained 6-SH-β-CD was dissolved into KH-590 and a small amount of H_2O_2 was added and stirred thoroughly. The natural bamboo material (60 mm × 20 mm × 6 mm) was immersed in the solution at room temperature. After soaking for 24 hours, take it out and dry it, the bamboo with a little bit of light white powder on the surface is ABS.

2.5. Fabrication of bonding specimens and testing of bonding strength

The CS-AD adhesive was uniformly coated on one side of the bamboo surface, the content was about 200 g/m^2, the coated part was lapped, the control lap area was 20 mm × 20 mm, and it was hot pressed for 6 min at 5 MPa under high temperature conditions. The effects of the ratio of adhesive components (CS: Hadc=1.2:1, 1:1, and 1:1.2), the solid content of CS-AD adhesive (5.8 %, 6.5 %, 7.4 %, and 8.5 %), and the hot-pressing temperatures (100, 120, 140, and 160 °C) on the bonding strength were explored by the controlled variable method, respectively. These bonded specimens were tested for bond strength according to GB /

T17657–2022 utilizing a microcomputer-controlled electromechanical universal testing machine (ETM10B, Shenzhen, China). The tensile speed was 2 mm/min and the specimens were stress-damaged within 30 s. Each specimen was made and tested ten times. The bonding strength of the hot-pressed specimens tested directly without any treatment is the dry strength, and the bonding strength of the hot-pressed bonded specimens tested after immersion in hot water (63 °C) and boiling water for 3 h is the hot water strength and boiling water strength, respectively.

2.6. Fourier transform infrared spectroscopy (FTIR)

The 1–2 mg 6-SH-β-CD and CS-AD adhesive samples and 200 mg of pure KBr were homogeneously ground and pressed in a mold to form clear slices, respectively. The samples were tested using an infrared spectrometer (Thermo Scientific Nicolet iS50). The wavenumber range was 4000–400 cm^{-1}, the resolution ratio was 4 cm-1, and the scanning times were 32. About the Attenuated Total Reflection-Fourier Transform Infrared Spectroscopy (ATR-FTIR) test method. The cut bamboo samples were put into the diamond ATR module, and other parameters were consistent with the above method.

2.7. Thermodynamic performance testing

Thermogravimetric analysis (TGA) and Derivative thermogravimetric analysis (DTG) were performed on CS-AD adhesive samples using TA Instruments Q50. The samples were heated from 30 °C to 800 °C at a rate of 10 °C/min and the ambient gas was nitrogen.

The CS-DA adhesive was tested using a NETZSCH DSC204F1. A specimen of known mass was placed in an aluminum crucible for compression, and the crucible with the specimen and the empty crucible was placed in a homogenizing furnace of the DSC instrument, the key parameters of the experiment were set to a starting temperature of 30°C, an ending temperature of 250°C, a ramp rate of 10 k/min, and an ambient gas of nitrogen.

2.8. X-ray photoelectron spectroscopy (XPS) testing

The CS-AD adhesive and ABS samples were tested using an XPS instrument (Thermo Fisher Scientific K-Alpha, USA). The spot size was 400 μm, the filament current was 6 mA, the operating voltage was 12 kV, the full-spectrum scanning energy was 150 eV in steps of 1 eV, and the narrow-band scanning energy was 50 eV in steps of 0.1 eV. The data were processed with Avantage analysis software.

2.9. X-ray diffraction (XRD) testing

The crystallinity of cyclodextrins and their inclusion complexes was analyzed by X-ray diffraction (XRD) using an UltimaIV diffractometer (Rigaku, Japan) at a voltage of 40 kV and a current of 40 mA with Cu Kα radiation (λ = 0.15406 nm) in the range of 5°- 60° and a scanning speed of 5°/min.

2.10. Contact angle test

The wettability of natural and activated bamboo surfaces was compared by contact angle/surface tension tester (CA, Dataphysics OCA20).

2.11. Humidity resistance test of specimens

The bonded specimens were placed in vacuum tanks of various salt solutions of different humidity for seven days. The room temperature was 10°C according to the humidity solution control chart.

3.2. Characterization of 6-SH-β-CD

The schematic diagram of the preparation process and chemical structure of 6-SH-β-CD are shown in Fig. 2a, and the physical photograph is shown in Fig. 2b. Mono-6-O-p-toluenesulfonyl-β-CD was synthesized by an aqueous phase method, which reduced the environmental pollution from organic solvents by using water as a solvent. β-CD has a low solubility in water, while tosyl chloride is insoluble in water, so prolonged stirring is required to bring the reactants into full contact. Hydrochloric acid produced during the reaction can be removed by adding NaOH aqueous solution. The chemical structures of β-CD, mono-6-O-tosyl-β-CD, and 6-SH-β-CD were characterized by FT-IR analysis, respectively, and the results are shown in Fig. 2c. For the spectrum of 6-SH-β-CD, the stretching vibration attributed to the C-S bond at 699 cm^{-1} confirmed the successful grafting of the sulfhydryl group, the stretching vibration of the S-H bond at 2573 cm^{-1} [39], and the vibrational absorption peaks of the cyclodextrin backbone at 800–650 cm^{-1} proved

that the cyclodextrin backbone was not destroyed [11]. The 6-SH-β-CD was further characterized by XPS, and the results are shown in Fig. 2d-g. A new S 2p peak was added to the XPS spectrum (Fig. 2d) of 6-SH-β-CD, which proves the introduction of S element. The appearance of C-S (285.5 eV), S-C (162.5 eV) and S-H (163.9 eV) bonds can be seen in the C 1 s (Fig. 2e) and S 2p (Fig. 2f) spectra of 6-SH-β-CD, which further indicates the successful preparation of 6-SH-β-CD [40].

3.3. Characterization of activated bamboo surface (ABS)

As shown in Fig. 3a, the ABS was prepared using a simple solvent immersion method by taking advantage of the dehydration condensation of silane coupling agent KH-590 with wood and the formation of disulfide bonds with sulfhydryl groups (-SH) in the adhesive. The photos of natural bamboo surface and activated bamboo surface are shown in Fig. 3b, a little bit of white powder is attached to the ABS surface. The chemical structures of NBS and ABS were characterized by FTIR
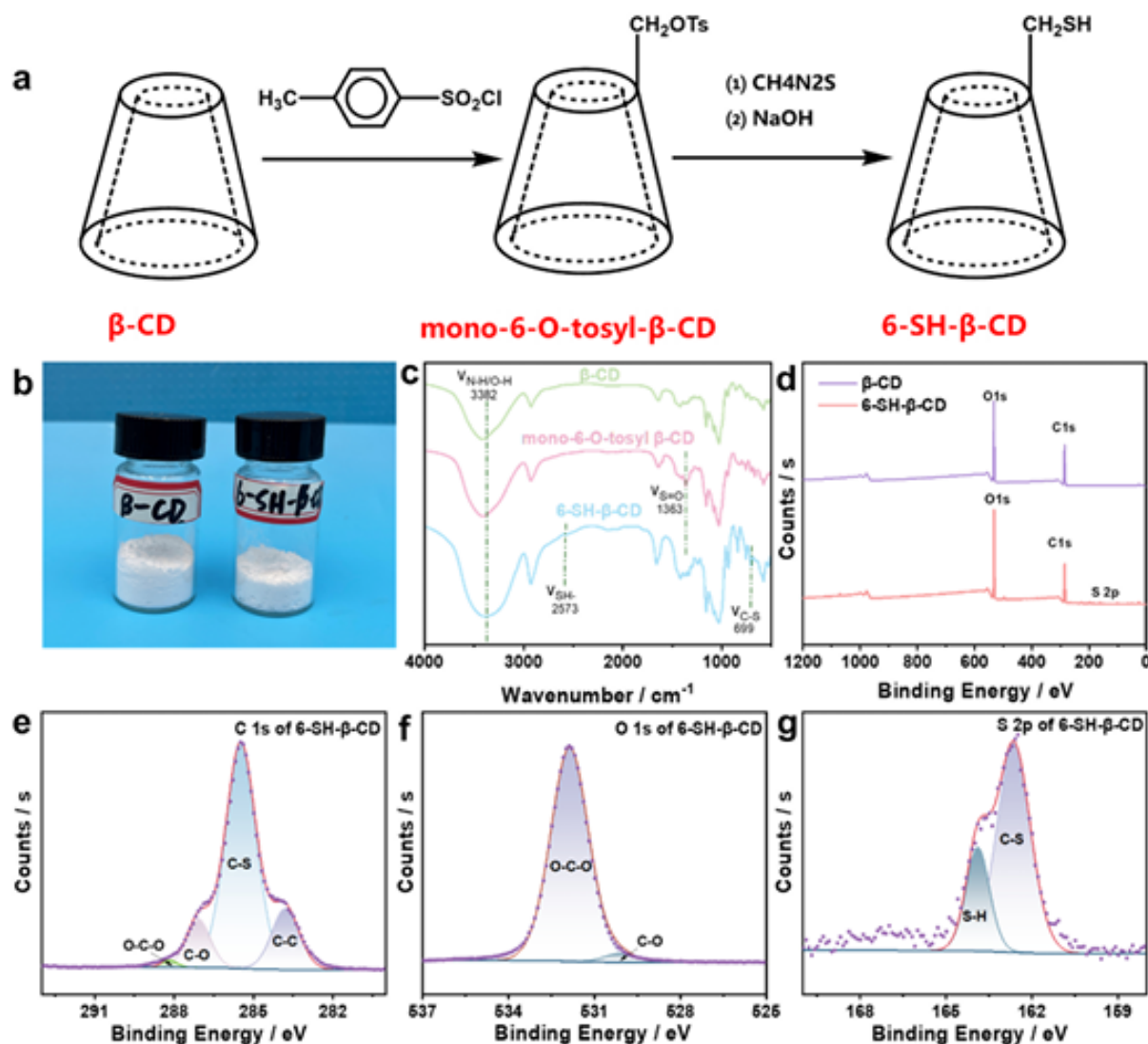

Fig. 2. (a) Schematic diagram of the preparation process and chemical structure of 6-mercapto-β-cyclodextrin. (b) Photos of β-CD and 6-SH-β-CD. (c) FTIR spectra of β-CD, mono-6-O-tosyl-β-CD, and 6-SH-β-CD. (d) XPS spectra of β-CD and 6-SH-β-CD. (e-g) High-resolution spectra of C 1 s, O 1 s, and S 2p of 6-SH-β-CD.

3.4. Analysis of thermodynamic properties of CS-AD adhesives

The CS-AD adhesives were tested by DSC. As shown in Fig. 4b, the CS: Hadc (1:1.2, 1:1, 1.2:1) adhesives with different ratios had obvious heat absorption peaks on the DSC curves. It can be observed that the integral areas of the DSC curves at different ratios are significantly different, implying different enthalpy changes. which can reflect the differences in the degree of curing of the samples to a certain extent. When CS: Hadc = 1:1, the peak area of the DSC curve for CS-AD is the largest, proving the largest enthalpy change, indicating the best degree of curing under this condition, and this result is consistent with that of the bonding strength data [34].

The thermal stability and thermal decomposition behavior of CS-Hadc adhesive were investigated by thermogravimetric analysis (TG). The TGA and DTG curves are shown in Fig. 4c and d, respectively. The maximum thermal degradation rates of CS and Hadc were 19.8 %/min (Tmax = 214 °C) and 13.3 %/min (Tmax = 268 °C), respectively, whereas the maximum thermal degradation rate of CS-Hadc adhesive was 16 %/min (Tmax = 203 °C). The results showed that the thermal properties of CS-Hadc were relatively stable.

3.5. Characterization of the inclusion complex (CS-AD-6-SH-β-CD)

During the bonding process, adamantane on the adhesive and cyclodextrin on the ABS will form an inclusion compound (CS-AD-6-SH-β-CD) by host-guest recognition at the bonding interface. Schematic diagram of the Supramolecular bonding interface is shown in Fig. 4a. Direct evidence for the detection of complexation of the host molecule 6-SH-β-CD with the guest in the powder state was obtained from the powder X-ray diffraction spectroscopy analysis. The diffractograms of CS-Hadc, 6-SH-β-CD and their inclusion complexes are shown in Fig. 4e. The characteristic peaks of CS-Hadc are 11.56, 13.48, 16.2, 17.42, 18.32, 20.88, 23.02, and 39.84, and those of 6-SH-β-CD are 12.12, 14.58, 15.62, 17.78, 18.84, 21.38, 23.8, 26.2, 31.78, 38.06, and the characteristic peak of the inclusion complex is 21.02. Such sharp and intense peaks of β-CD and adamantane move, disappear, or become less intense in a complex form due to the subject wrapping the guest in the hydrophobic cavity of β-CD [41]. This structural change may lead to a decrease in crystallinity in the XRD patterns. The differences observed between these patterns confirm the formation of a new solid phase. As shown in Fig. S2, the samples were characterized using UV spectroscopy. In the compounds formed by 6-SH-β-CD and sulfhydryl silane coupling agent (KH-590), there are a large number of saturated chemical bonds, such as carbon-carbon single bonds (C-C), carbon-hydrogen single bonds (C-H), silicon-carbon single bonds (Si-C), and silicon-oxygen single bonds (Si-O), etc. The electrons in these single bonds undergo a process of σ-σ leaps from the bonding σ orbitals to the antibonding σ orbitals. The electrons in these single bonds undergo a jump from the bonding σ-orbitals to the antibonding σ-orbitals, which requires a higher energy. According to the inverse relationship between energy and wavelength, high energy corresponds to short wavelength, so the absorption peaks of such leaps usually appear in the far-ultraviolet region, i.e., the wavelength range of less than 200 nm. When cellulose-grafted adamantane forms a host-guest inclusion complex with cyclodextrin, the interactions between the host and the guest through van der Waals forces, hydrogen bonding, and other interactions result in a change in the charge distribution within the molecule. This change in charge distribution may lead to a redistribution of the electron cloud density of the molecule so that the energy level difference between the highest occupied molecular orbital and the lowest unoccupied molecular orbital of the molecule decreases. A decrease in the energy level difference means that the energy required for the electron to jump is reduced, corresponding to a longer wavelength of absorbed light, and thus a red shift.

3.6. Testing and analysis of bonding properties and water resistance

The bonding strength is a key indicator for assessing the performance of composites, which directly affects their structural stability and durability, and is important for ensuring the robustness of composites in service. The effects of solid content, hot pressing temperature, mass ratio of CS to Hadc, and the construction of supramolecular adhesive interfaces on the adhesive bonding properties were investigated using the control variable method. During the application process, it was found that CS-AD adhesive has better wettability on ABS than NBS. Therefore, the dynamic contact angle was used to verify this phenomenon. Through the dynamic contact angle data (Fig. 4f) and the contact angle photographs (Fig. 4g), it can be clearly found that the contact angle of CS-AD adhesive on ABS is relatively smaller, indicating a better wettability, which is beneficial to realize high-performance bonding.

Firstly, the effects of solid content, CS/Hadc mass ratio and temperature on the bonding properties were explored separately under the condition of unconstructed supramolecular bonding interface (NBS as substrate), and the results are shown in Fig. 5a-c. The experimental results showed that the best bonding performance was achieved when the adhesive solid content was 5.8 %, the optimal ratio of CS to Hadc was 1:1, and the hot-pressing temperature was 160 °C without constructing a supramolecular bonding interface. The dry, hot, and boiling water strengths of the bamboo specimens reached 7.8, 6.4 and 4.9 MPa, respectively. In addition, a new set of experiments was conducted under the condition of constructing an activated interface (AWS as the substrate), and the results are shown in Fig. 5d-f. The experimental results showed that the optimal adhesive solid content was 6.5 % and the optimal ratio of CS to Hadc was 1:1, which were mostly consistent with the results of the study without constructing the activated interface condition. The difference is that the bonding strength is significantly improved, and the dry, hot, and boiling water bonding strengths of the bamboo specimens reached 10.7 MPa, 7.2 MPa, and 6.4 MPa, respectively. The Bonding performance improved by about 30 % overall. The disconnected specimens in Fig. 5g and h showed that even though the specimens were treated with boiling water, the bamboo breakage rate was still high, again demonstrating the robust bonding performance of the prepared bamboo composites.

Based on the above studies, the strategy of constructing supramolecular bonding interfaces was further applied to wood bonding. Tests were conducted on poplar and beech wood, and Fig. 6a-c show the stress-strain curves of dry, hot, and boiling water strengths, respectively. The specific bonding strengths of poplar and beech are shown in Fig. 6d and e, respectively. Through the feedback of the bonding strength data, it can be clearly concluded that the construction of supramolecular bonding interface can effectively enhance the bonding performance and realize the breakthrough of the bonding performance on the basis of the original. To verify the stability of the bonding system, the prepared specimens were placed in different relative humidity environments for 7 days and the bonding strength was tested immediately after removal. As shown in Fig. 6f, the results showed an overall decreasing trend in bonding performance with increasing humidity, especially for the specimens with unconstructed supramolecular bonding interface. However, when the supramolecular bonding interface was constructed, the humidity had almost no effect on the bamboo specimens, and even when the humidity exceeded more than 90 %, the bonding strength could still reach more than 8 MPa. The effect of UV aging on bonding performance of bonded specimens was investigated, the results are shown in Fig. 6g. The bonded specimens constructed with supramolecular bonded interface had better UV aging resistance. In addition, the bonded bamboo specimens were immersed in petroleum ether (PE), ethyl acetate (EA), ethanol (EtOH) and NaCl solutions for 40 h, and the effects of treatments with different solvents on the bonding properties were investigated, and the results were shown in Fig. S3, which showed that the decrease of the bonding properties was not obvious, indicating that it had a certain degree of solvent resistance. The high temperature
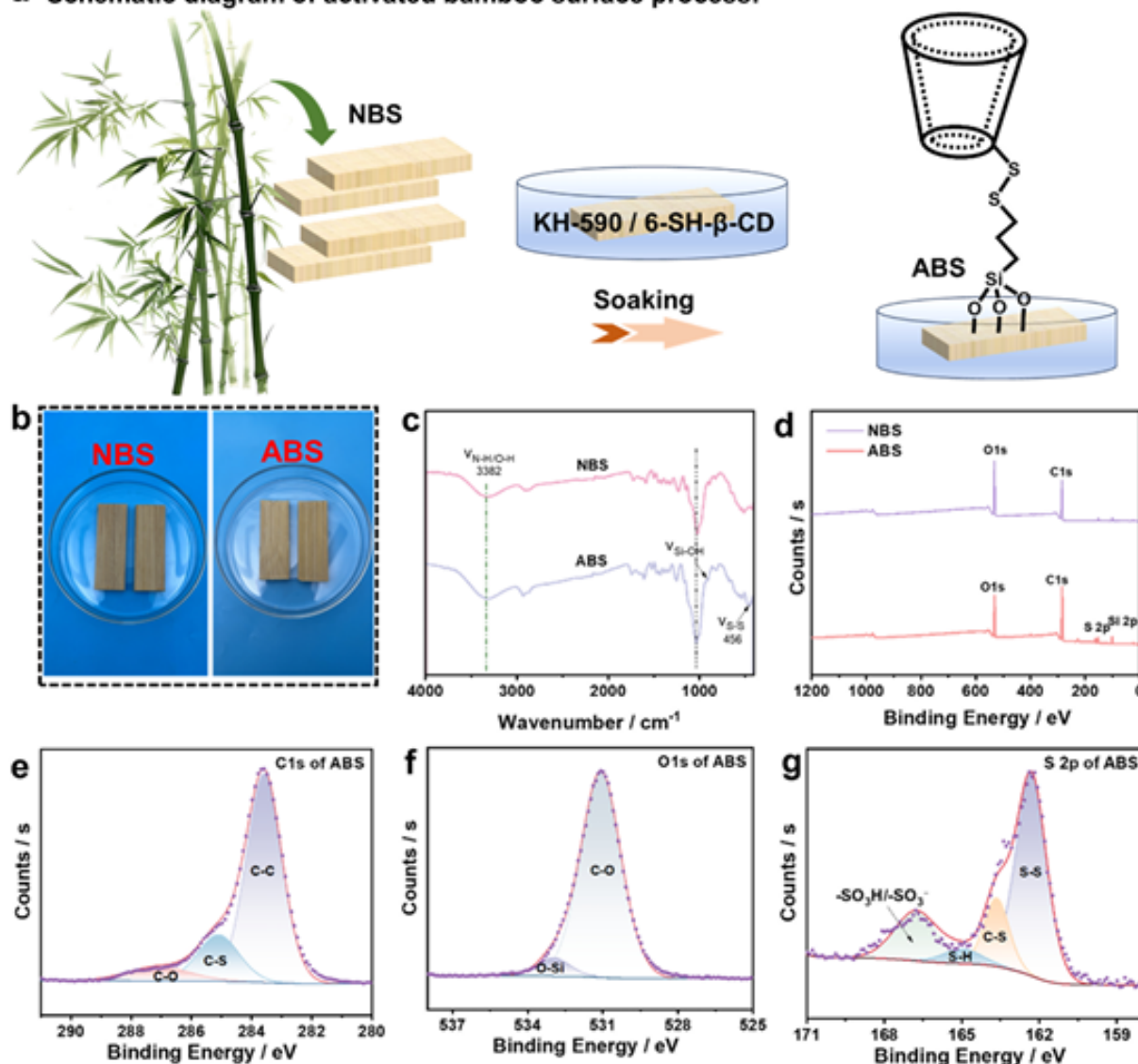
Fig. 3. (a) Schematic diagram of the preparation process of activated bamboo surface (ABS). (b) The photo of natural bamboo surface (NBS) and ABS. (c) FTIR spectra of NBS and ABS. (d) XPS spectra of NBS and ABS. (e-g) High-resolution spectra of C 1 s, O 1 s, and S 2p of ABS.

analysis, and the results are shown in Fig. 3c, while both of them have a peak near 3382 cm^{-1} for O-H bond stretching vibration. For ABS, a vibrational signal of S-S bond appears at 456 cm^{-1} and a vibrational signal of Si-O bond appears at 918 cm^{-1}. The peak at 1025 cm^{-1} was shifted to the vicinity of 1042 cm^{-1}, which was attributed to the silane coupling agent altering the polarity or the hydrogen bonding network on the surface of the wood, resulting in the shift of the original peak position, which was manifested as an apparent blue shift. And the peak signals increased and broadened, which was due to the reaction between silane coupling agent and hydroxyl group (-OH) in wood to generate Si-O-C bonding and the overlap of the C-O-C expansion vibration peaks of wood itself. The successful grafting of KH-590 with 6-SH-β-CD was demonstrated. Further analysis of ABS by XPS showed the appearance of S element, C-S, S-C, and S-S bonds in the elemental composition (Fig. 3d), C 1 s (Fig. 3e) and S 2p (Fig. 3g) spectra, which likewise

proved the successful grafting of KH-590 and 6-SH-β-CD on the bamboo surface [39]. In addition, it is possible that the sulfhydryl group is partially over-oxidized by hydrogen peroxide to produce sulfonic acid (-SO$_3$H), and thus will appear as -SO$_3$H/-SO$_3^-$ signals in the S 2p high-resolution spectrum. The O-Si signal in the O 1 s (Fig. 3f) spectra of ABS may be attributed to the chemical reaction between KH-590 and the hydroxyl group on the bamboo surface, and also to the signal of KH-590 itself. In the high-resolution spectrum of Si 2p (Fig. S1) of ABS, a Si-O-C signal appeared, indicating the bonding between silane and wood. The attachment phenomenon of white powder on the surface of ABS shows that the linkage between KH-590 and the surface of bamboo may also have a mechanical interlocking effect formed by physical filling [31].
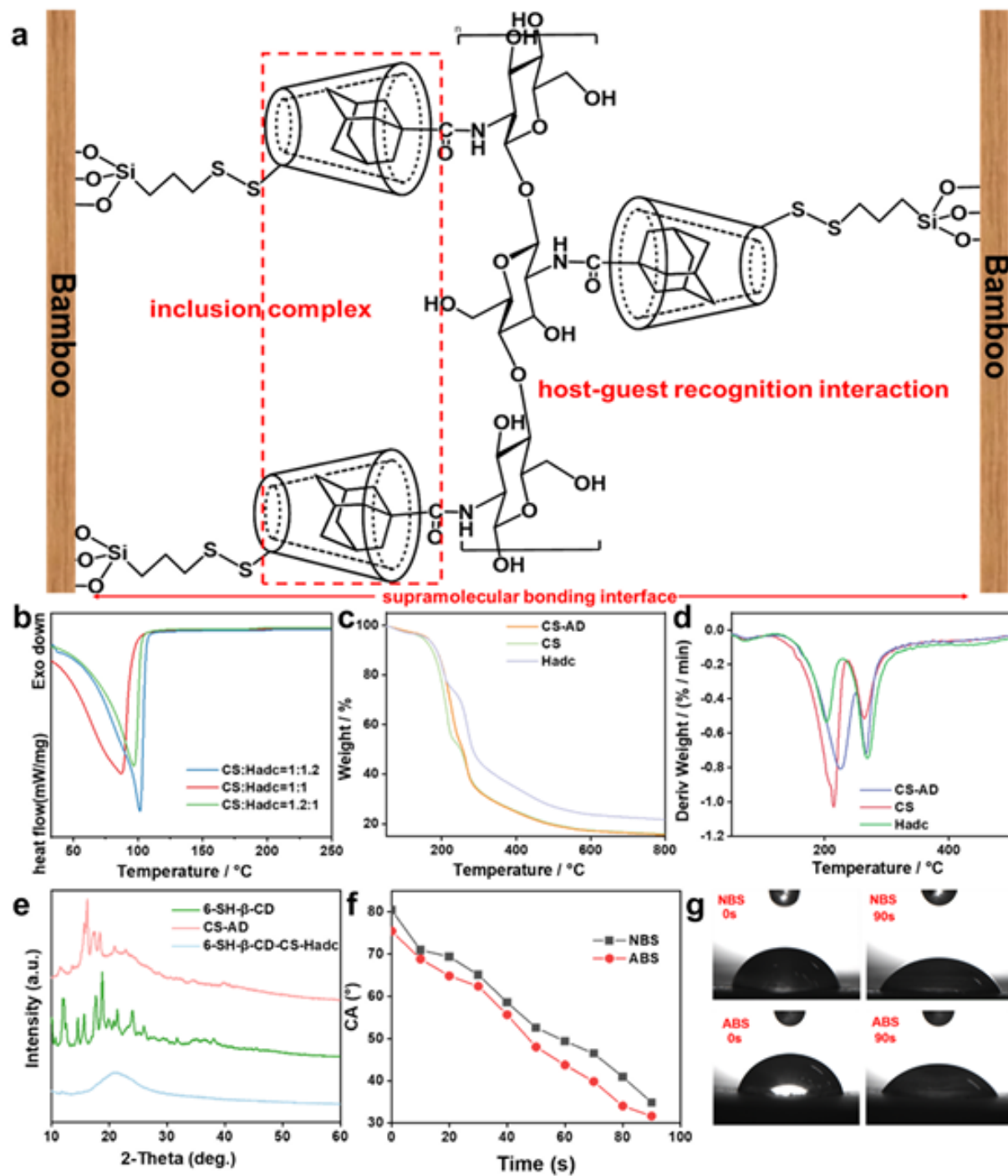
Fig. 4. (a) Schematic diagram of the Supramolecular bonding interface. (b) DSC curves of CS-AD adhesive at different ratio. TG (c) and DTG (d) curves of CS, Hadc, and CS-AD adhesive. (e) XRD spectra of 6-SH-β-CD, CS-AD, and inclusion complex. (f) Dynamic contact angle curves for NBS and ABS. (f) Contact angle photos for NBS and ABS.
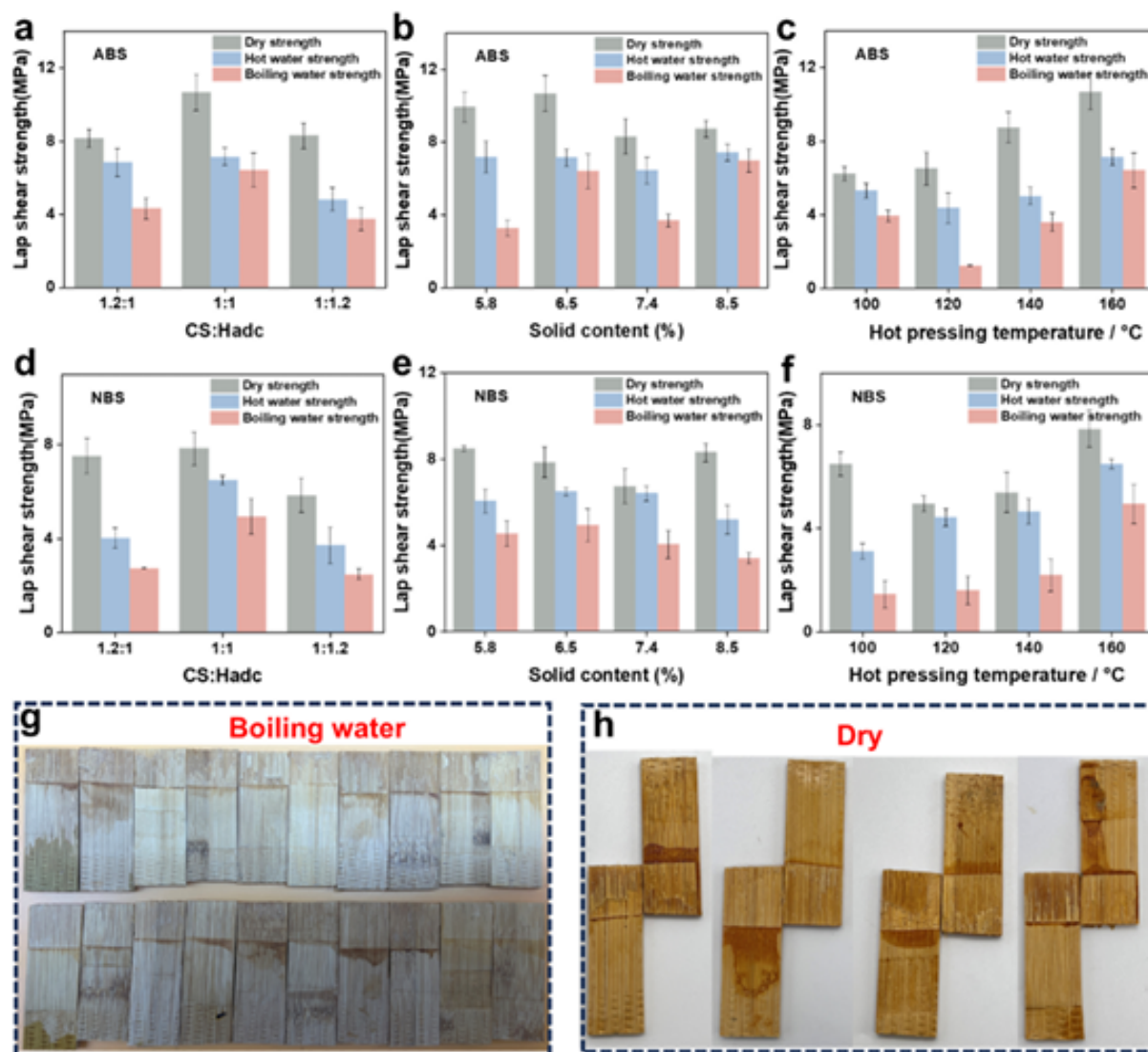
Fig. 5. The effects of adhesive ratio (a), solid content (b), and hot-pressing temperature (c) on the performance of bonding under the condition of using ABS as the substrate. The effects of adhesive ratio (d), solid content (e), and hot-pressing temperature (f) on the performance of bonding under the condition of using NBS as the substrate. (g) Photographs of bamboo bonded specimens pulled off after soaking in boiling water for 3 h. (h) Photographs of bamboo bonded specimens pulled off in the dry state.

resistance test was conducted by placing the bonded specimens in an oven at 200 °C for 1 h and then removing them to cool down to room temperature and reheat again, and so on for three times to test the mechanical properties. The freeze-thaw cycle test was conducted by placing the bonded specimens in a refrigerator at −18 °C for 1 h and then removing them to restore to room temperature and refreeze again, and so on for three times to test the mechanical properties. The experimental results are shown in Fig. S4, where the effect of low temperature is less compared to the effect of high temperature on the bonding properties. The size of bonded specimen and photos of the fixture during the testing process are shown in Fig. 6h. To generalize the results, the strategy was applied to bond Polystyrene (PS), PMMA, Al, PVC, PTFE, PET, glass and other substrates. The bonding results as shown in Fig. 6i demonstrate that it is practical to realize the breakthrough in bonding performance by constructing supramolecular bonding interface, and the

detailed bonding strengths are shown in Fig. S5-Fig. S6. As shown in Fig. 6j, the bonded specimen was demonstrated for the bonding performance to show the robustness of the bonded specimen. A bonded specimen of bamboo with a bonding area of 20 mm × 10 mm can easily pull up a strong adult weighing 121.9 kg and remain intact.

4. Conclusions

In this work, the chitosan grafted adamantane guest molecule was used as an adhesive, while the cyclodextrin host was modified on the bamboo surface, and a supramolecular bonding interface was formed through the host-guest recognition between cyclodextrin and adamantane during the bonding process, which realized a further breakthrough based on the original bonding performance. After the construction of the supramolecular bonding interface, the bonding

[31] T. Liu, G. Du, H. Yang, K. Ni, H. Su, H. Wen, L. Yang, Cellulose-based ultrastrong wood adhesive and composites constructed through "sandwich" profile bonding interface, Compos. Part B Eng. 271 (2024) 111169, https://doi.org/10.1016/j.compositesb.2023.111169.

[32] W. Kang, K. Ni, H. Su, H. Yang, X. Zhang, H. Li, L. Yang, Glued-bamboo composite based on a highly cross-linked cellulose-based adhesive and an epoxy functionalized bamboo surface, Int. J. Biol. Macromol. 270 (2024) 132500, https://doi.org/10.1016/j.ijbiomac.2024.132500.

[33] H. Su, G. Du, X. Ren, C. Liu, Y. Wu, H. Zhang, L. Yang, High-performance bamboo composites based on the chemical bonding of active bamboo interface and chitosan, Int. J. Biol. Macromol. 244 (2023) 125345, https://doi.org/10.1016/j.ijbiomac.2023.125345.

[34] T. Liu, Y. Shao, X. Zhang, J. Wan, G. Du, L. Yang, X. Ran, A chitosan-based adhesive with high flame retardancy and superior bonding strength fabricated by interface engineering, Int. J. Biol. Macromol. 305 (2025) 140984, https://doi.org/10.1016/j.ijbiomac.2025.140984.

[35] G.W. Chen, S.Y. Li, H.J. Liu, H. Wang, R. Sun, J.F. Ge, Fluorescence enhancement of cyanine/hemicyanine dyes with adamantane as an auxochrome through host–guest inclusion with methylated cyclodextrin in water, Spectrochim. Acta A Mol. Biomol. Spectrosc. 329 (2025) 125540, https://doi.org/10.1016/j.saa.2024.125540.

[36] D. Iudin, M.J. van Steenbergen, R. Masereeuw, B.G. van Ravensteijn, T. Vermonden, Shrinkable hydrogels through host–guest interactions: a robust approach to obtain tubular cell-laden scaffolds with small diameters, Adv. Funct. Mater. (2024) 2416522, https://doi.org/10.1002/adfm.202416522.

[37] E.I. Popescu, L. Aricov, S. Mocanu, I. Matei, E. Hristea, R. Baratoiu, G. Ionita, Subtle influence on alginate gel properties through host–guest interactions between covalently appended cyclodextrin and adamantane units, N. J. Chem. 45 (18) (2021) 8083–8091, https://doi.org/10.1039/D1NJ01278A.

[38] J. Park, Y. Sasaki, Y. Ishii, S. Murayama, K. Ohshiro, K. Nishiura, Y. Takashima, Leaf-inspired host–guest complexation-dictating supramolecular gas sensors, ACS Appl. Mater. Interfaces 15 (33) (2023) 39777–39785, https://doi.org/10.1021/acsami.3c04395.

[39] C. Yin, J. Wang, G. Du, K. Ni, H. Wang, T. Liu, L. Yang, Developing a water-resistant cellulose-based wood adhesive based on dual dynamic Schiff base and disulfide bonds, Ind. Crops Prod. 209 (2024) 118011, https://doi.org/10.1016/j.indcrop.2023.118011.

[40] Y.L. Wang, M. Stanzione, H. Xia, G.G. Buonocore, E. Fortunati, S. Kaciulis, M. Lavorgna, Effect of mercapto-silanes on the functional properties of highly amorphous vinyl alcohol composites with reduced graphene oxide and cellulose nanocrystals, Compos. Sci. Technol. 200 (2020) 108458, https://doi.org/10.1016/j.compscitech.2020.108458.

[41] M. Kundu, S. Saha, M.N. Roy, Evidences for complexation of β-cyclodextrin with some amino acids by ¹H NMR, surface tension, volumetric investigations and XRD, J. Mol. Liq. 240 (2017) 570–577, https://doi.org/10.1016/j.molliq.2017.05.123.
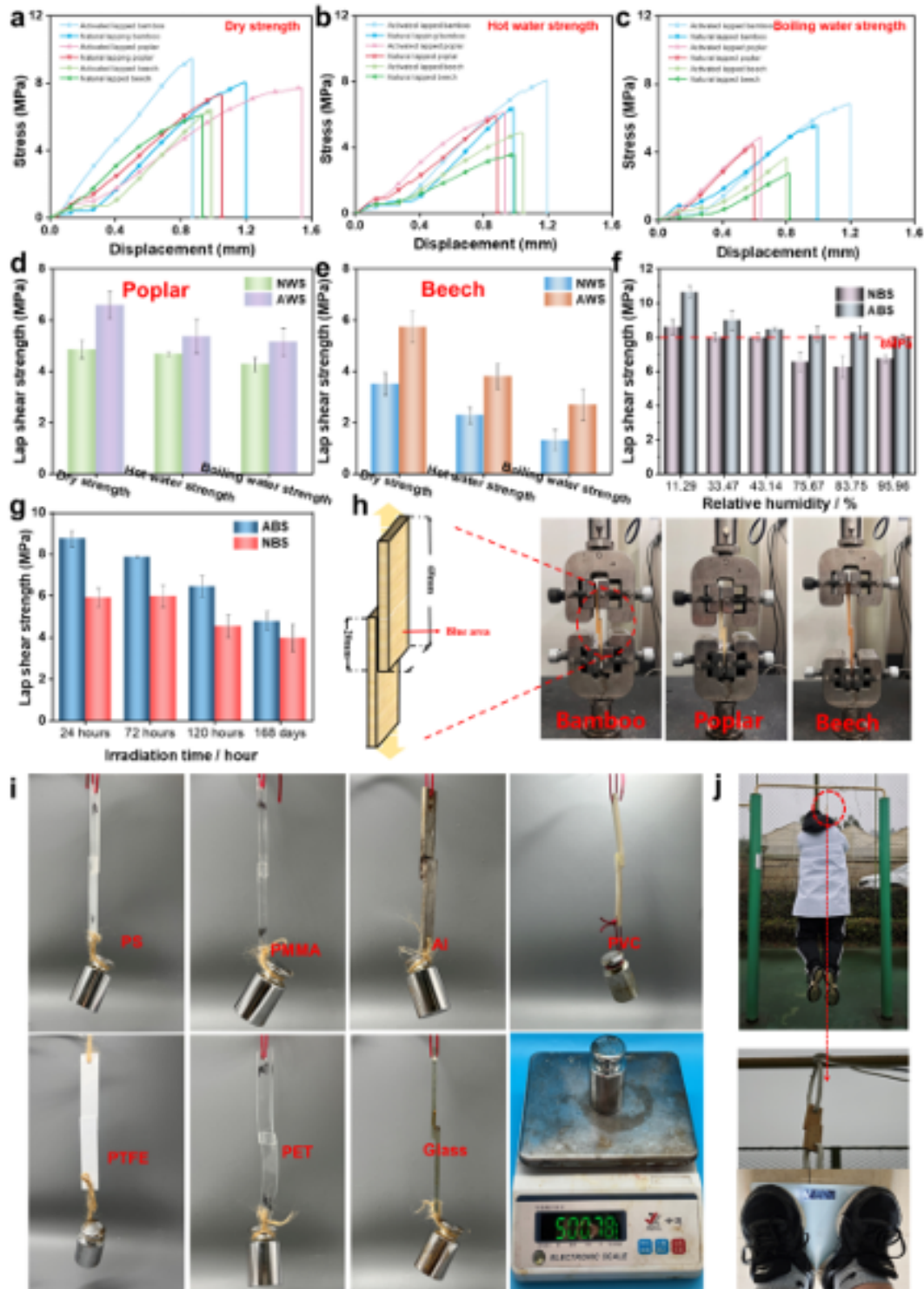
Fig. 6. Stress-strain curves for dry strength (a), hot water strength (b), and boiling water strength (c) of bonded specimens of wood (poplar and beech) and bamboo. The bonding strength of poplar (d) and beech (e). (h) Size of bonded specimen and photos of the fixture during the testing process. (i) Effective bonding of substrates such as Polystyrene (PS), PMMA, Al, PVC, PTFE, PET, glass, etc. can be realized through the construction of supramolecular bonding interface. (j) Photograph of a bonded bamboo specimen bearing the weight of a strong adult and the weight of the participants in the test.

10

strength of the bamboo bonded specimens increased by about 30 % in general, and the dry, hot and boiling water strengths reached 10.7 MPa, 7.2 MPa and 6.4 MPa, respectively. In addition, this strategy is not only suitable for bamboo bonding, but also for bonding PMMA, PS, PVC, Al, glass, PET, wood and many other metallic and non-metallic substrates. The current work combines macrocyclic supramolecular interaction forces with bonding technology, realized a breakthrough in bonding performance, broke the barriers of traditional bonding technology, and contributed to the development of high-performance bonding technology and the improvement of bonding theory.

CRediT authorship contribution statement

Yang Long: Writing – review & editing, Supervision, Funding acquisition, Conceptualization. **Li Jun:** Funding acquisition. **Du Guanben:** Funding acquisition. **Wei Renzhong:** Investigation. **Liu Tongda:** Writing – review & editing, Visualization, Funding acquisition. **Zhao Rui:** Writing – original draft, Methodology, Investigation. **Xue Weibing:** Writing – original draft, Methodology, Formal analysis. **Lu Tonghua:** Investigation. **Liu Rong:** Data curation. **Ran Xin:** Funding acquisition.

Declaration of Competing Interest

The authors declare that they have no known competing financial interests or personal relationships that could have appeared to influence the work reported in this paper.

Acknowledgements

Appendix A. Supporting information

Supplementary data associated with this article can be found in the online version at doi:10.1016/j.colsurfa.2025.136765.

Data availability

Data will be made available on request.

References

[1] H. Sun, X. Li, H. Li, D. Hui, M. Gaff, R. Lorenzo, Nanotechnology application on bamboo materials: a review, Nanotechnol. Rev. 11 (1) (2022) 1670–1695, https://doi.org/10.1515/ntrev-2022-0101.

[2] Z. Ba, H. Luo, J. Guan, J. Luo, J. Gao, S. Wu, R.O. Ritchie, Robust flexural performance and fracture behavior of TiO₂ decorated densified bamboo as sustainable structural materials, Nat. Commun. 14 (1) (2023) 1234, https://doi.org/10.1038/s41467-023-36939-6.

[3] L.S. Rukaibawi, S.L. Omairey, G. Károlyi, A numerical anatomy-based modelling of bamboo microstructure, Constr. Build. Mater. 308 (2021) 125036, https://doi.org/10.1016/j.conbuildmat.2021.125036.

[4] J. Parr, L. Sullivan, B. Chen, G. Ye, W. Zheng, Carbon bio-sequestration within the phytoliths of economic bamboo species, Glob. Change Biol. 16 (10) (2010) 2661–2667, https://doi.org/10.1111/j.1365-2486.2009.02118.x.

[5] J. Shi, H. Yu, W. Qin, W. Yang, X. Zhuang, F. Rao, Z. Ban, Fabrication of a new bamboo composite with large-size high-quality flattened surface, Ind. Crops Prod. 209 (2024) 117953, https://doi.org/10.1016/j.indcrop.2023.117953.

[6] J. Wang, R. Wang, X. Ji, C. Jin, Y. Yan, Enhancing and toughening bamboo interfacial bonding strength by reactive hyperbranched polyethyleneimine modified phenol formaldehyde resin adhesive, J. Mater. Res. Technol. 26 (2023) 8213–8228, https://doi.org/10.1016/j.jmrt.2023.09.176.

[7] W. Liu, L. Liao, H. Jiang, Z. Li, Fracture properties of bamboo fibrous composites: a systematic review, J. Build. Eng. 97 (2024) 110672, https://doi.org/10.1016/j.jobe.2024.110672.

[8] W. Zhang, C. Wang, S. Gu, H. Yu, H. Cheng, G. Wang, Physical-mechanical properties of bamboo fiber composites using filament winding, Polymers 13 (17) (2021) 2913, https://doi.org/10.3390/polym13172913.

[9] Q. Zhou, Y. Xu, P. Liu, Y. Qin, H. Zhang, Mechanical properties of energy sustainable round bamboo-phosphogypsum composite floor slabs, J. Build. Eng. 76 (2023) 107192, https://doi.org/10.1016/j.jobe.2023.107192.

[10] Z. Huang, H. Künzel, M. Krus, W. Zhang, Three-dimensional tests on hygric properties of laminated bamboo and bamboo scrimber, J. Build. Eng. 56 (2022) 104712, https://doi.org/10.1016/j.jobe.2022.104712.

[11] R. Zhao, T. Liu, X. Ran, J. Li, G. Du, L. Yang, Imitation expansion bolts structural bonding interface: enhancing the bonding properties of bamboo composites through host-guest molecular recognition, Chem. Eng. J. 500 (2024) 156771, https://doi.org/10.1016/j.cej.2024.156771.

[12] L. Xia, Q. Chen, M. Jiang, J. Yuan, J. Xie, In-situ surface liquefaction strategy for bamboo bonding with high-performance, Compos. Part B Eng. 297 (2025) 112288, https://doi.org/10.1016/j.compositesb.2025.112288.

[13] X. Zhang, K. Ni, T. Liu, C. Yin, H. Yang, X. Ran, J. Wan, An effective approach for lignin-based bamboo adhesive preparation via swelling crosslinking, Int. J. Biol. Macromol. 300 (2025) 140361, https://doi.org/10.1016/j.ijbiomac.2025.140361.

[14] X. Liu, W. Gu, K. Wang, Q. Gao, H. Chen, S.Q. Shi, J. Li, Preparation of biomimetic functionalized hierarchical bamboo fibers for reinforcing plant protein-based adhesives, Int. J. Adhes. Adhes. 120 (2023) 103280, https://doi.org/10.1016/j.ijadhadh.2022.103280.

[15] H. Shi, H. Huo, H. Yang, H. Li, J. Shen, J. Wan, L. Yang, Cellulose-based dual-network conductive hydrogel with exceptional adhesion, Adv. Funct. Mater. 34 (48) (2024) 2408560, https://doi.org/10.1002/adfm.202408560.

[16] T. Huang, L. Liu, J. Qian, Z. Zhu, Z. Xie, H. Yang, L. Yang, Gallic acid modified aminated cellulose integrated polyethylenimine to construct a phenol-amine chemical network for bonding wood, Ind. Crops Prod. 221 (2024) 119333, https://doi.org/10.1016/j.indcrop.2024.119333.

[17] Z. Tang, X. Lin, M. Yu, J. Yang, S. Li, A.K. Mondal, H. Wu, A review of cellulose-based catechol-containing functional materials for advanced applications, Int. J. Biol. Macromol. 266 (2024) 131243, https://doi.org/10.1016/j.ijbiomac.2024.131243.

[18] Z. Tang, M. Zhao, N. Li, H. Xiao, Q. Miao, M. Zhang, H. Wu, Self-healing, reusable and conductive cellulose nanocrystals-containing adhesives, Colloids Surf. A Physicochem. Eng. Asp. 643 (2022) 128797, https://doi.org/10.1016/j.colsurfa.2022.128797.

[19] X. Zhang, X. Zhang, L. Cai, J. Li, P. Song, J. Li, Q. Gao, Strong and antistatic biomass adhesive for wood-based composites with electrostatic discharge protection function, Ind. Crops Prod. 219 (2024) 119055, https://doi.org/10.1016/j.indcrop.2024.119055.

[20] X. Zhang, C. Long, X. Zhu, X. Zhang, J. Li, J. Luo, Q. Gao, Preparation of strong and thermally conductive, spider silk-inspired, soybean protein-based adhesive for thermally conductive wood-based composite, ACS Nano 17 (19) (2023) 18850–18863, https://doi.org/10.1021/acsnano.3c03782.

[21] W. Kong, J. Ren, Bonding plant fibers with uncondensed lignin as adhesive, Adv. Fiber Mater. 6 (2024) 335–337, https://doi.org/10.1007/s42765-024-00389-6.

[22] C. Yang, H. Su, G. Du, X. Ren, Y. Wu, H. Zhang, L. Yang, Aldehyde-amine crosslinked starch-based high-performance wood adhesive, Eur. J. Wood Prod. 81 (6) (2023) 1557–1568, https://doi.org/10.1007/s00107-023-01985-w.

[23] Y. Chen, X. Huang, G. Wang, H. Liu, X. Lin, P. Song, Q. Gao, Preparation of a long-term mildew resistant and strong soy protein adhesive via constructing multiple crosslinking networks, Chem. Eng. J. 492 (2024) 152045, https://doi.org/10.1016/j.cej.2024.152045.

[24] S. Chen, Y. Chen, Z. Wang, H. Chen, D. Fan, Renewable bio-based adhesive fabricated from a novel biopolymer and soy protein, RSC Adv. 11 (19) (2021) 11724–11731, https://doi.org/10.1039/D1RA00766A.

[25] Z. Kou, Y. Sha, M. Liu, G. Zhang, J. Wang, M. Zhang, Y. Zhou, Bio-based and recyclable adhesives based on β-hydroxyester bonds and hydrogen bonds via molecular dynamics simulation, J. Mater. Chem. A 13 (7) (2025) 5119–5129, https://doi.org/10.1039/D4TA06980C.

[26] Z. Liang, J. Xue, Q. Yan, Y. Sun, S. Luo, Y. Zhu, S. Zhang, Advanced dual-cross-linking strategy for upgrading formaldehyde-free olefin adhesives, Nano Lett. 25 (7) (2025) 2931–2938, https://doi.org/10.1021/acs.nanolett.4c06353.

[27] H. Zhang, P. Liu, S.M. Musa, C. Mai, K. Zhang, Dialdehyde cellulose as a bio-based robust adhesive for wood bonding, ACS Sustain. Chem. Eng. 7 (12) (2019) 10452–10459, https://doi.org/10.1021/acssuschemeng.9b00801.

[28] H. Chen, Q. Wu, X. Ren, X. Zhu, D. Fan, A fully bio-based adhesive with high bonding strength, low environmental impact, and competitive economic performance, Chem. Eng. J. 494 (2024) 153198, https://doi.org/10.1016/j.cej.2024.153198.

[29] H. Su, G. Du, H. Yang, Y. Wu, S. Liu, K. Ni, L. Yang, Novel ultrastrong wood bonding interface through chemical covalent crosslinking of aldehyde-amine, Ind. Crops Prod. 189 (2022) 115800, https://doi.org/10.1016/j.indcrop.2022.115800.

[30] T. Liu, G. Du, Y. Wu, C. Liu, H. Yang, K. Ni, L. Yang, Activated wood surface and functionalized cellulose co-building strong chemical wood bonding performance, Carbohydr. Polym. 305 (2023) 120573, https://doi.org/10.1016/j.carbpol.2023.120573.

11